Timing with Dirty Templates for Low-Resolution Digital UWB Receivers

Huilin Xu and Liuqing Yang, *Senior Member, IEEE*

***Abstract*— As a rapid timing synchronization technique for ultra-wideband (UWB) communications, the timing with dirty templates (TDT) technique effectively collects the multipath energy even when the channel is unknown [7]. In this paper, we investigate TDT algorithms for digital UWB receivers with low-resolution analog-to-digital converters (ADC). Different from the original TDT in [7] for analog UWB receivers, our digital TDT synchronizers here can avoid the ultra-wideband analog delay elements which are difficult to implement at the IC level. Our analysis and simulations show that the (non)data-aided digital TDT algorithms remain operational even when the ADC resolution is very low.**

***Index Terms*— Analog-digital conversion, multipath channels, synchronization, signal detection, timing.**

I. Introduction

In UWB impulse radio systems, information is conveyed by low-power impulse-like waveforms. Therefore, timing synchronization for UWB systems is more challenging than for conventional narrowband systems. To facilitate rapid synchronization in analog UWB systems, TDT algorithms were recently proposed [7]. By correlating two consecutive symbol-long segments of the received waveform, these algorithms can effectively collect the multipath energy even when the channel and the spreading codes are both unknown.

In this paper, we adapt the TDT algorithms to low-resolution digital UWB receivers with 2- or 3-bit analog-to-digital converters (ADC). Unlike their analog counterparts in [7], our digital TDT algorithms have to operate in the presence of both the additive Gaussian noise and considerable quantization errors. We prove that the (non)data-aided digital TDT algorithms remain operational even when the ADC resolution is very low, and without the knowledge of either the spreading codes or the multipath propagation channel. Our simulations also verify that the resolution of the ADCs has very little effect on the synchronization performance.

Our results here have very practical implications: TDT-based timing synchronization algorithms can be carried out at digital UWB receivers using very-low-resolution ADCs, without invoking the analog UWB delay lines that are difficult to implement at the IC level. In addition, we will show that our digital TDT algorithms rely on digital operations which can be further exploited to enhance the receiver flexibility, in comparison with analog TDT.

Manuscript received August 3, 2006; revised November 1, 2006; accepted January 26, 2007. The associate editor coordinating the review of this letter and approving it for publication was D. Huang. This work is supported by the National Science Foundation under Grant ECS-0621879. Part of the results in this paper was presented at the IEEE International Conference on Ultra-Wideband, Waltham, MA, Sept. 24-27, 2006.

The authors are with the Department of Electrical and Computer Engineering, University of Florida, P.O. Box 116130, Gainesville, FL 32611, USA (e-mail: xuhl@ufl.edu, lqyang@ece.ufl.edu).

Digital Object Identifier 10.1109/TWC.2008.060542.

II. System Model

Consider an impulse radio UWB system, where every information symbol is transmitted over a T_s period that consists of N_f frames. During each frame of duration T_f, a data-modulated short pulse $p(t)$ of duration $T_p \ll T_f$ is transmitted. Though TDT has been shown to be capable of handling pulse position modulation (PPM) and multi-user applications [7], here we will focus on a peer-to-peer scenario with pulse amplitude modulation (PAM). Specifically, the transmitted signal is

$$v(t) = \sqrt{\mathcal{E}} \sum_{k=0}^{\infty} s(k) \cdot p_T(t - kT_s) \,, \tag{1}$$

where $\mathcal{E}$ is the energy per pulse, $s(k)$ is the kth information symbol taking values $\{\pm 1\}$ and $p_T(t) = \sum_{n=0}^{N_f-1} c_{ds}(n) \cdot p(t - nT_f - c_{th}(n)T_c)$ denotes the transmitted symbol-long waveform. Notice that $p_T(t)$ can be regarded as the symbol-level pulse shaper which accounts for the time-hopping (TH) and/or direct-sequence (DS) spreading via $c_{th}(n)$ and $c_{ds}(n)$, respectively.

Let $g(t-\tau_0)$ denote the multipath channel with propagation delay τ_0[1]. Then, the received waveform can be expressed as

$$r(t) = \sqrt{\mathcal{E}} \sum_{k=0}^{\infty} s(k) \cdot p_R(t - kT_s - \tau_0) + \eta(t) \,, \tag{2}$$

where $p_R(t) := p_T(t) \star g(t)$ is the aggregate symbol-long received waveform with $\star$ denoting convolution, and $\eta(t)$ represents the zero-mean additive white Gaussian noise (AWGN) with power spectral density $\mathcal{N}_0/2$. As in [7], we assume that the support of $p_R(t)$ is bounded by T_s; that is, there is no inter-symbol interference (ISI). However, it is worth emphasizing that inter-frame interference (IFI) is allowed and can be significant especially when TH is present.

The received signal $r(t)$ is filtered by a matched-filter $p(-t)$ and sampled every T_t seconds with a low-resolution ADC (see e.g., [6]). Without loss of generality, we assume that $T_s = N_T T_t$. Then, the received waveform becomes [c.f. (2)]

$$u(n) = \sqrt{\mathcal{E}} \sum_{k=0}^{\infty} s(k) \tilde{p}_R(n - kN_T - N_{\tau_0}) + \zeta(n) + e(n), \tag{3}$$

where $N_{\tau_0} := \lfloor \tau_0/T_t \rfloor$ is the propagation delay, $\tilde{p}_R(n), n \in [0, \ldots, N_T - 1]$, are the ADC outputs corresponding to the symbol-long waveform $p_R(t), t \in [0, T_s)$, $\zeta(n)$ is the AWGN with variance $\mathcal{N}_0/2$, and $e(n)$ is the quantization error due to the finite ADC resolution.

[1]As many existing timing algorithms, the TDT-based ones here are also blind to timing offsets that are integer multiples of the symbol duration. Therefore, we assume that τ_0 is upper bounded by T_s.

III. Digital TDT Algorithms

In this section, we will introduce the digital TDT algorithms for estimating N_{τ_0}. Following the idea of the dirty templates [7], these algorithms rely on successive symbol-long signal groups each consisting of N_T samples $u(n)$. Specifically, with $N_\tau \in [0, \ldots, N_T - 1]$ denoting the candidate time shift, the kth signal group consists of samples $\{u(n+N_\tau)\}_{n=kN_T}^{(k+1)N_T-1}$. The $2k$th and the $(2k+1)$st groups are then correlated to yield the symbol-rate samples as follows:

$$x(k;N_\tau) = \sum_{n=0}^{N_T-1} u(n+2kN_T+N_\tau) \times u(n+(2k-1)N_T+N_\tau), \quad \forall k \in [1,+\infty) . \tag{4}$$

Notice that, in this correlation, the two groups are serving as correlator *templates* for each other.

In the absence of the AWGN and the quantization error, applying the Cauchy-Schwartz [1] inequality to (4), we obtain

$$x^2(k;N_\tau) \le \sum_{n=0}^{N_T-1} u^2(n+2kN_T+N_\tau) \times \sum_{n=0}^{N_T-1} u^2(n+(2k-1)N_T+N_\tau) . \tag{5}$$

Following the proof in [7], we know that the equality in (5) holds for any sequence of information symbols if and only if $N_{\tau_0} = N_\tau$; that is, $x^2(k;N_\tau)$ reaches its maximum when $N_{\tau_0} = N_\tau$, when both the AWGN and the quantization error are absent.

With an analog UWB receiver, this observation has been proved to remain valid even in the presence of AWGN [7]. In the contrast, for digital UWB receivers with low-resolution ADCs, the interference component also includes the quantization error which is correlated with the noise-free part of the received analog waveform. Next, we will analyze the statistical characteristics of the noise at the ADC output and prove that the observation of (5) holds true even in the presence of both the AWGN $\zeta(n)$ and the quantization error $e(n)$.

A. Noise Analysis

Let $\tilde{N}_{\tau_0} := [N_{\tau_0} - N_\tau]_{N_T}$ denote the residual synchronization error, where $[a]_b$ represents the modulo operation on a with base b. Using (3), the kth symbol-rate sample defined in (4) can be explicitly expressed as

$$x(k;N_\tau) = \Big(s(2k-2)\mathcal{E}_A(\tilde{N}_{\tau_0}) + s(2k)\mathcal{E}_B(\tilde{N}_{\tau_0})\Big) \times s(2k-1) + \xi(k;N_\tau), \tag{6}$$

where $\mathcal{E}_A(\tilde{N}_{\tau_0}) := \mathcal{E} \cdot \sum_{n=N_T-\tilde{N}_{\tau_0}}^{N_T-1} \tilde{p}_R^2(n)$, $\mathcal{E}_B(\tilde{N}_{\tau_0}) := \mathcal{E} \cdot \sum_{n=0}^{N_T-\tilde{N}_{\tau_0}-1} \tilde{p}_R^2(n)$ and the noise term $\xi(k;N_\tau) := \xi_1(k;N_\tau) + \xi_2(k;N_\tau)$ consists of two parts

$$\begin{aligned}\xi_1(k;N_\tau) :=& \sum_{n=0}^{\tilde{N}_{\tau_0}-1} \sqrt{\mathcal{E}}\,(s(2k-2)\nu(n+2kN_T+N_\tau) \\ &+ s(2k-1)\nu(n+(2k-1)N_T+N_\tau))\,\check{p}(n) \\ &+ \sum_{n=0}^{\tilde{N}_{\tau_0}-1} \nu(n+(2k-1)N_T+N_\tau)\nu(n+2kN_T+N_\tau) , \\ \xi_2(k;N_\tau) :=& \sum_{n=\tilde{N}_{\tau_0}}^{N_T-1} \sqrt{\mathcal{E}}\,(s(2k-1)\nu(n+2kN_T+N_\tau) \\ &+ s(2k)\nu(n+(2k-1)N_T+N_\tau))\,\check{p}(n) \\ &+ \sum_{n=\tilde{N}_{\tau_0}}^{N_T-1} \nu(n+(2k-1)N_T+N_\tau)\nu(n+2kN_T+N_\tau) ,\end{aligned}$$

with $\nu(n) := \zeta(n) + e(n)$ and $\check{p}(n) := \tilde{p}_R([n+N_T-\tilde{N}_{\tau_0}]_{N_T})$. Unlike the high-resolution ADC, the uniform quantization error assumption does not hold for low-resolution ADCs [5], [6]. Specifically, the assumption that the quantization error is uniform and independent of the input signal is *not* valid. For digital UWB receivers with low-resolution ADCs, we found that:

Proposition 1: The expected values of the noise terms $\xi_1(k;N_\tau)$ and $\xi_2(k;N_\tau)$ are

$$\begin{aligned} m_1(k;N_\tau) &:= \mathrm{E}\{\xi_1(k;N_\tau)\} \\ &= s(2k-2)s(2k-1)m_1(N_\tau) \\ \text{and} \quad m_2(k;N_\tau) &:= \mathrm{E}\{\xi_2(k;N_\tau)\} \\ &= s(2k-1)s(2k)m_2(N_\tau), \end{aligned}$$

respectively, where $m_1(N_\tau)$ and $m_2(N_\tau)$ are independent of k and $m_\xi := m_1(N_\tau) + m_2(N_\tau)$ is a constant independent of N_τ. Their variances $\sigma_1^2(N_\tau) := \mathrm{var}\{\xi_1(k;N_\tau)\}$ and $\sigma_2^2(N_\tau) := \mathrm{var}\{\xi_2(k;N_\tau)\}$ are also independent of k, and $\sigma_\xi^2 := \sigma_1^2(N_\tau) + \sigma_2^2(N_\tau)$ is a constant.

Proof: See Appendix. ■

Using Proposition 1, and by the central limit theorem, $x(k;N_\tau)$ in (6) can be approximated as a Gaussian random variable with variance $\mathrm{var}\{x(k;N_\tau)\} = \sigma_\xi^2$ and mean $\mathrm{E}\{x(k;N_\tau)\} = s(2k-1)(s(2k-2)\bar{\mathcal{E}}_A(\tilde{N}_{\tau_0}) + s(2k)\bar{\mathcal{E}}_B(\tilde{N}_{\tau_0}))$, where $\bar{\mathcal{E}}_A(\tilde{N}_{\tau_0}) := \mathcal{E}_A(\tilde{N}_{\tau_0}) + m_1(N_\tau)$ and $\bar{\mathcal{E}}_B(\tilde{N}_{\tau_0}) := \mathcal{E}_B(\tilde{N}_{\tau_0}) + m_2(N_\tau)$. Accordingly, the mean-square of $x(k;N_\tau)$ can be obtained as

$$\begin{aligned}\mathrm{E}\{x^2(k;N_\tau)\} &= \mathrm{E}^2\{x(k;N_\tau)\} + \mathrm{var}\{x(k;N_\tau)\} \\ &= \frac{1}{2}\mathcal{E}_D^2(\tilde{N}_{\tau_0}) + \frac{\mathcal{E}_R^2}{2} + \sigma_\xi^2,\end{aligned} \tag{7}$$

where $\mathcal{E}_R := \bar{\mathcal{E}}_A(\tilde{N}_{\tau_0}) + \bar{\mathcal{E}}_B(\tilde{N}_{\tau_0})$ is a constant and $\mathcal{E}_D(\tilde{N}_{\tau_0}) := \bar{\mathcal{E}}_A(\tilde{N}_{\tau_0}) - \bar{\mathcal{E}}_B(\tilde{N}_{\tau_0})$. With proper setting of the scale of the low-resolution ADC, both $\bar{\mathcal{E}}_A(\tilde{N}_{\tau_0})$ and $\bar{\mathcal{E}}_B(\tilde{N}_{\tau_0})$ are positive $\forall \tilde{N}_{\tau_0} \in [0, \ldots, N_T-1]$. Accordingly, when $\tilde{N}_{\tau_0} = 0$, $\mathcal{E}_D(\tilde{N}_{\tau_0})$ reaches its maximum value $\mathcal{E}_R$. This proves that, even in the presence of both the AWGN and the quantization error, the mean-square of the symbol-rate samples $x(k;N_\tau)$ is maximized when synchronization is achieved. Based on this principle, the digital version of the TDT algorithms can be established, in both *nondata-aided* (NDA) and *data-aided* (DA) modes.

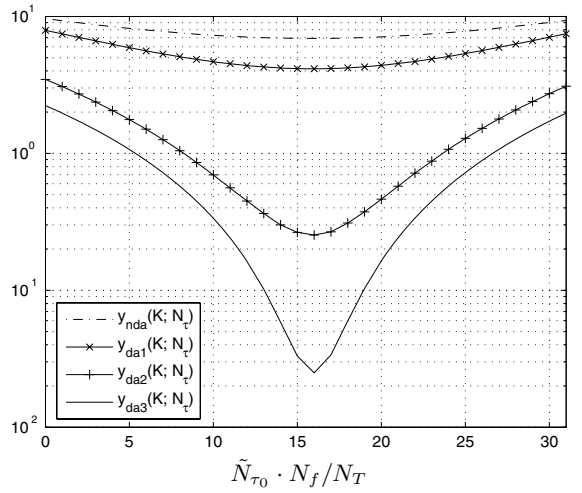

Fig. 1. Means of $y_{nda}(K;N_\tau)$, $y_{da1}(K;N_\tau)$, $y_{da2}(K;N_\tau)$ and $y_{da3}(K;N_\tau)$ (K=16, N_f=32, $\mathcal{E}/\mathcal{N}_0 = 5$dB).

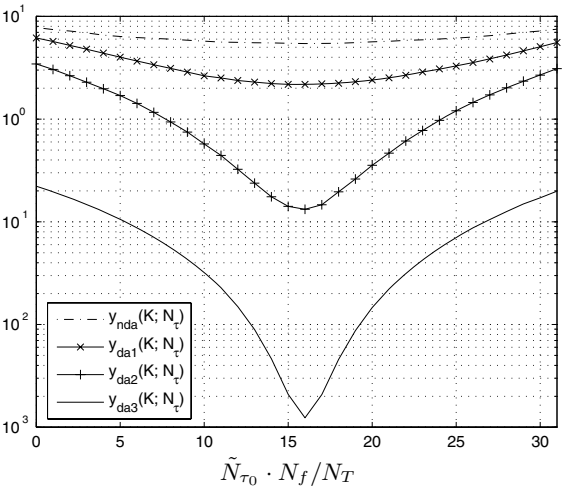

Fig. 2. Variances of $y_{nda}(K;N_\tau)$, $y_{da1}(K;N_\tau)$, $y_{da2}(K;N_\tau)$ and $y_{da3}(K;N_\tau)$ (K=16, N_f=32, $\mathcal{E}/\mathcal{N}_0 = 5$dB).

B. Digital TDT Algorithms

A general expression of the timing offset (propagation delay) estimator is given by:

$$\hat{N}_{\tau_0} = \arg\max_{N_\tau} y(K;N_\tau)\ , \tag{8}$$

where $y(K;N_\tau)$ is the objective function. Depending on the operating mode of the estimator, the objective function $y(K;N_\tau)$ can be formed differently, as we will specify next.

In the NDA mode, the objective function is the mean-square of K successive symbol-rate samples (see (4))

$$y_{nda}(K;N_\tau) = \frac{1}{K} \sum_{k=1}^{K} \left(\sum_{n=2kN_T}^{(2k+1)N_T-1} u(n+N_\tau)\cdot u(n+N_\tau-N_T) \right)^2 . \tag{9}$$

Notice that (9) is essentially the sample mean counterpart of the ensemble expression in (7). Hence, the maximum of $y_{nda}(K;N_\tau)$ will give the estimate of N_{τ_0}, even when TH and/or DS codes are present and the UWB multipath channel remains unknown.

One major advantage of $y_{nda}(K;N_\tau)$ is that it can be applied to *any* information symbol sequence transmitted. However, the timing acquisition process can be expedited when the following training sequence is employed [7]:

$$s(k) = (-1)^{\lfloor k/2 \rfloor}\ . \tag{10}$$

Using this sequence, the objective function can still be formulated as in (9). To distinguish from the NDA mode, we will denote it with $y_{da1}(K;N_\tau)$ for the DA mode.

In fact, with the training sequence in (10), the *averaging* and *squaring* operations can be exchanged to obtain more accurate estimates of the *mean-square* of $x(k;N_\tau)$ in (7). Such variants give rise to the following formulations of the objective function

$$y_{da2}(K;N_\tau) = \left(\frac{1}{K} \sum_{k=1}^{K} \sum_{n=2kN_T}^{(2k+1)N_T-1} u(n+N_\tau)\cdot u(n+N_\tau-N_T) \right)^2 \tag{11}$$

and

$$y_{da3}(K;N_\tau) = \left(\sum_{n=0}^{N_T-1} \bar{u}(n+N_\tau)\cdot \bar{u}(n+N_\tau-N_T) \right)^2 , \tag{12}$$

where $\bar{u}(n) := K^{-1}\sum_{k=1}^{K}(-1)^k u(n+2kN_T)$.

From their definitions, we can obtain the means and variances of these objective functions:

$$\begin{aligned} m_{y_{nda}}(K;N_\tau) &= \tfrac{1}{2}\mathcal{E}_D^2(\tilde{N}_{\tau_0}) + \tfrac{\mathcal{E}_R^2}{2} + \sigma_\xi^2 \\ m_{y_{da1}}(K;N_\tau) &= \mathcal{E}_D^2(\tilde{N}_{\tau_0}) + \sigma_\xi^2 \\ m_{y_{da2}}(K;N_\tau) &= \mathcal{E}_D^2(\tilde{N}_{\tau_0}) + \tfrac{1}{K}\sigma_\xi^2 \\ m_{y_{da3}}(K;N_\tau) &= \mathcal{E}_D^2(\tilde{N}_{\tau_0}) + \sigma_\xi^2 \end{aligned} , \tag{13}$$

and

$$\begin{aligned} \sigma^2_{y_{nda}}(K;N_\tau) &= \tfrac{2\sigma_\xi^2}{K}\left[\mathcal{E}_D^2(\tilde{N}_{\tau_0}) + \mathcal{E}_R^2 + \sigma_\xi^2\right] \\ &\quad + \tfrac{4}{K}\bar{\mathcal{E}}_A^2(\tilde{N}_{\tau_0})\bar{\mathcal{E}}_B^2(\tilde{N}_{\tau_0}) \\ \sigma^2_{y_{da1}}(K;N_\tau) &= \tfrac{2\sigma_\xi^2}{K}\left[2\mathcal{E}_D^2(\tilde{N}_{\tau_0}) + \sigma_\xi^2\right] \\ \sigma^2_{y_{da2}}(K;N_\tau) &= \tfrac{2\sigma_\xi^2}{K}\left[2\mathcal{E}_D^2(\tilde{N}_{\tau_0}) + \tfrac{\sigma_\xi^2}{K}\right] \\ \sigma^2_{y_{da3}}(K;N_\tau) &= 2\sigma_\xi^2\left[2\mathcal{E}_D^2(\tilde{N}_{\tau_0}) + \sigma_\xi^2\right] \end{aligned} , \tag{14}$$

where $\sigma_\xi^2 := \frac{\sigma_1^2(N_\tau)}{K} + \frac{\sigma_2^2(N_\tau)}{K^2}$, and $\xi_1(k;N_\tau)$ and $\xi_2(k;N_\tau)$ are assumed to be independent in deriving the mean and variance of $y_{da3}(K;N_\tau)$. The means and variances of the four objective functions are plotted in Figs. 1 and 2 with $K = 16$ and $\frac{\mathcal{E}}{\mathcal{N}_0} = 5$dB. The means of the objective function, with peaks appearing at $\tilde{N}_{\tau_0} = 0$, suggest that one can find the correct timing by peak-picking. The variances are dependent on the timing offset $\tilde{N}_{\tau_0}$, as indicated by (14).

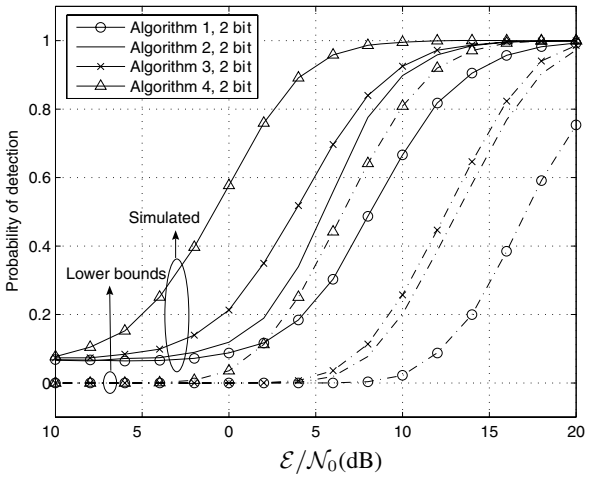

Fig. 3. Probabilities of detection and lower bounds for *Algorithm 1-4* ($K = 16$).

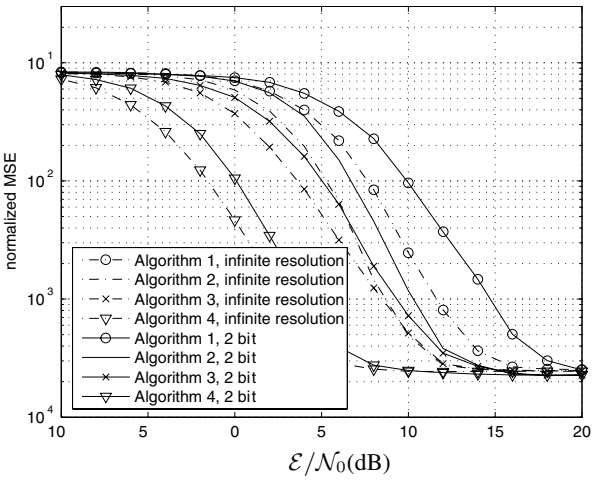

Fig. 5. Normalized MSE for 2-bit ADC and infinite-resolution ADC ($K = 16$).

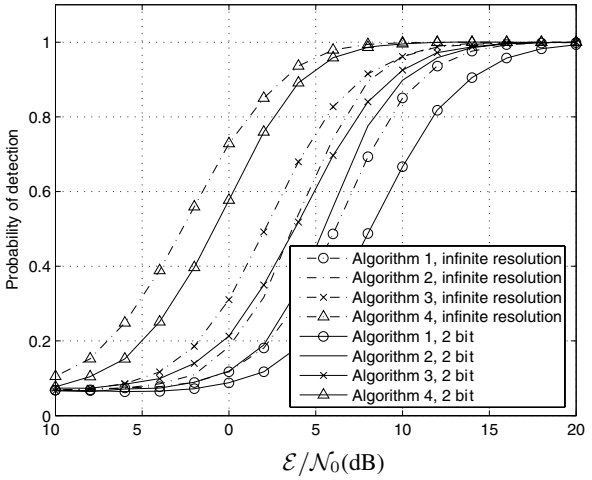

Fig. 4. Probabilities of detection for 2-bit ADC and infinite-resolution ADC ($K = 16$).

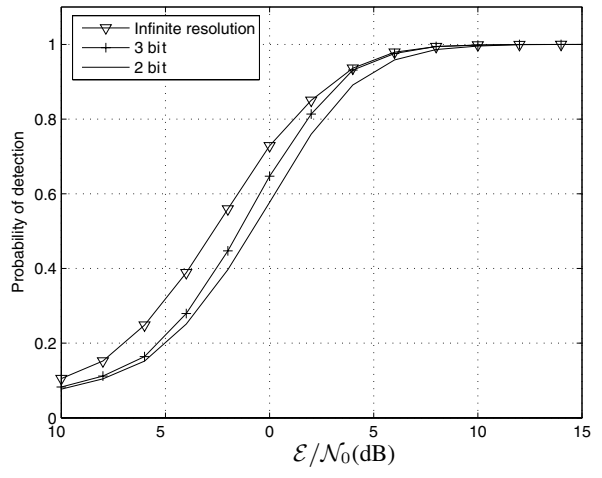

Fig. 6. Probabilities of detection for *Algorithm 4*: 2-bit ADC, 3-bit ADC and infinite-resolution ADC ($K = 16$).

It should be noted that, instead of the analog delay lines entailed by the analog TDT algorithms in [7], the delay operation here can be easily implemented with registers. All the digital operations that follow, including the correlation and peak-picking, can be carried out by general-purpose hardware using digital signal processing (DSP) chips and/or field programmable gate arrays (FPGA) that are readily available (see, e.g., [4]).

IV. Performance Comparisons

In this section, we will compare the acquisition performances of these digital TDT algorithms in a coarse timing setup. In this setup, instead of estimating the true N_{τ_0}, the receiver partitions the symbol duration N_T into N_i intervals each of duration $N_t := N_T/N_i$. The timing acquisition then amounts to finding n^* that maximizes the objective function among possible candidates $n \in [0, N_i - 1]$. In other words, $\widehat{n^*} = \arg\max_{n\in[0,N_i-1]} y(K; nN_t)$.

To predict the performance of TDT algorithms, we will adopt a lower bound on the probability of detection

$$\underline{P_d} = \prod_{n\neq n^*} Q\left(\frac{m_y(K;n^*N_t) - m_y(K;nN_t)}{\sqrt{\sigma_y^2(K;n^*N_t) + \sigma_y^2(K;nN_t)}}\right). \quad (15)$$

This bound has been proved to be universally tighter than the union bound [3], [7]. From (13), (14) and (15), we deduce that for all four digital TDT algorithms, the lower bounds decrease as K increases. This implies that, similar to the analog TDT (see [7]), the performance of digital TDT algorithms can be improved by increasing K.

From (13) and (14), together with the fact that $\sigma_{\bar{\xi}}^2 = \frac{\sigma_1^2(N_\tau)}{K} + \frac{\sigma_2^2(N_\tau)}{K^2} < \frac{\sigma_\xi^2}{K} = \frac{\sigma_1^2(N_\tau)+\sigma_2^2(N_\tau)}{K}$, it is straightforward to obtain $(m_{y_{nda}}(K;n^*N_t) - m_{y_{nda}}(K;nN_t)) < (m_{y_{da1}}(K;n^*N_t) - m_{y_{da1}}(K;nN_t)) = (m_{y_{da2}}(K;n^*N_t) - m_{y_{da2}}(K;nN_t)) = (m_{y_{da3}}(K;n^*N_t) - m_{y_{da3}}(K;nN_t))$ and $\sigma_{ynda}^2(K;nN_t) > \sigma_{yda1}^2(K;nN_t) > \sigma_{yda2}^2(K;nN_t) > \sigma_{yda3}^2(K;nN_t)$ (see also Fig. 2). Accordingly, the lower bounds corresponding to different objective functions satisfy

$\underline{P}_{d,nda} < \underline{P}_{d,da1} < \underline{P}_{d,da2} < \underline{P}_{d,da3}$. This indicates that the DA-TDT outperforms the NDA-TDT and that, even with the same training pattern, the DA estimators can have different performances with slightly different objective functions. However, unlike the analog TDT synchronizers where the performance improvement comes at the price of increased complexity, all DA-TDT algorithms here have nearly the same complexity, thanks to the digital implementation. Therefore, the digital TDT with objective function $y_{nda3}(K;N_\tau)$ is preferable when pilot symbols are employed.

Besides the type of the timing estimator, the ADC resolution Δ (a.k.a. quantization step size) can also affect the acquisition performance. It is difficult to derive the analytical relationship between Δ and the acquisition performance, due to the complexity of the probability density function (PDF) of the quantization error. However, to gain some intuition, we notice that, as the resolution of the ADC increases, the quantization error becomes approximately uniformly distributed on $[-\Delta/2, \Delta/2]$. The variance of the aggregate noise then approaches $(\mathcal{N}_0/2+\Delta^2/12)$, where $\mathcal{N}_0/2$ comes from the AWGN and $\Delta^2/12$ from the quantization error [5]. Therefore, the smaller Δ, the smaller the noise variance and the better the acquisition performance.

V. Simulations

In our simulations, we will refer to the TDT algorithms with objective functions y_{nda}, y_{da1}, y_{da2} and y_{da3} as *Algorithms 1-4*, respectively. These algorithms are tested using the IEEE802.15.3a channel model CM1 [2]. The UWB pulse is the second derivative of the Gaussian function, and has unit energy and duration $T_p \approx 1$ns. The sampling frequency of the low-resolution ADC is 1GHz. The maximum scale of the ADC V_m is set as the maximum magnitude of the transmitted pulse $p(t)$. We use $N_f = 32$, $T_f = 40$ns and a random TH code uniformly distributed over $[0, N_c - 1]$ with $N_c = 40$ and $T_c = 1$ns. Notice that with these parameters, severe IFI is inevitable. To avoid ISI, we set $c_{N_f-1} = 0$ for the last frame of each symbol. In all simulations, only frame-level coarse timing is performed.

In Fig. 3, we observe that the bounds predict the relative performances of *Algorithms 1-4* very well. Fig. 4 and 5 show the comparison of the synchronizers with a 2-bit ADC and an ideal ADC of infinite resolution. At all SNR values, the acquisition performance improves from *Algorithm 1* to *Algorithm 4*. In addition, even with the same training pattern, *Algorithm 4* outperforms the other two DA-TDT algorithms. More importantly, with a low-resolution digital UWB receiver, this is achieved without increasing the complexity, as opposed to the analog TDT in [7]. Fig. 6 illustrates the effects of the ADC resolution. As the ADC resolution increases from 2 and 3 bits to infinity, the probability of detection improves only slightly.

VI. Conclusions

In this paper, we proposed the digital TDT algorithms with low-resolution ADCs. The major advantage of these digital TDT algorithms is that they can avoid the ultra-wideband analog delay lines, and exploit the flexible digital implementation. Our noise analysis justifies the applicability of the digital TDT algorithms. The simulations show that, with a low-resolution ADC, we can realize the timing estimator with very low complexity. Equally important is that, compared to the TDT using ADC of infinite resolution, the low-resolution ADC only induces very small performance degradation.

Appendix: Proof of Proposition 1

To prove Proposition 1, we will start with the mean of $\xi_1(k;N_\tau)$. Given the transmitted symbols $s(2k)$, $s(2k-1)$ and $s(2k-2)$, the mean of $\xi_1(k;N_\tau)$ is:

$$\begin{aligned}\mathrm{E}\{\xi_1(k;N_\tau)\} = &\sum_{n=0}^{\tilde{N}_{\tau_0}-1} \sqrt{\mathcal{E}}\,(s(2k-2)\mathrm{E}\{e(n+2kN_T+N_\tau)\}\\ &+ s(2k-1)\mathrm{E}\{e(n+(2k-1)N_T+N_\tau)\})\,\check{p}(n)\\ &+ \sum_{n=0}^{\tilde{N}_{\tau_0}-1} \mathrm{E}\{e(n+(2k-1)N_T+N_\tau)\}\mathrm{E}\{e(n+2kN_T+N_\tau)\}.\end{aligned}$$

To find the mean of the quantization error $e(n+kN_T+N_\tau)$, $\forall k$ and $n \in [0,\ldots,\tilde{N}_{\tau_0}-1]$, we notice that its corresponding input $\gamma(n;k;N_\tau) := \sqrt{\mathcal{E}}s(k-1)\check{p}(n) + \zeta(n+kN_T+N_\tau)$ is Gaussian distributed with mean $\sqrt{\mathcal{E}}s(k-1)\check{p}(n)$ and variance $\mathcal{N}_0/2$. For a b-bit roundoff ADC of uniform resolution, the resolution is $\Delta = 2V_m/2^b$. Applying the quantization error analysis in [5], the mean of $e(n+kN_T+N_\tau)$ is given by

$$\begin{aligned}\mathrm{E}\{e(n+kN_T+N_\tau)\} = &\sum_{l=1}^{\infty} \frac{\Delta}{\pi l}(-1)^l \exp\left(-\frac{\pi^2 l^2 \mathcal{N}_0}{\Delta^2}\right)\\ &\times \sin\left(\frac{2\pi l\sqrt{\mathcal{E}}s(k-1)\check{p}(n)}{\Delta}\right).\end{aligned}$$

Notice that, for binary PAM, the transmitted symbol $s(k) \in \{\pm 1\}$. Hence, $\mathrm{E}\{e(n+kN_T+N_\tau)\}$, $\forall n \in [0,\ldots,\tilde{N}_{\tau_0}-1]$ can be re-expressed as $\mathrm{E}\{e(n+kN_T+N_\tau)\} = s(k-1)m_e(n,N_\tau)$, where $m_e(n,N_\tau)$ is a function of $\check{p}(n)$ and is independent of the information symbols. As a result, the means of $\xi_1(k;N_\tau)$ and $\xi_2(k;N_\tau)$ can be obtained as

$$\begin{aligned}\mathrm{E}\{\xi_1(k;N_\tau)\} &= s(2k-2)s(2k-1)m_1(N_\tau);\\ \mathrm{E}\{\xi_2(k;N_\tau)\} &= s(2k-1)s(2k)m_2(N_\tau),\end{aligned}$$

where $m_1(N_\tau) := \sum_{n=0}^{\tilde{N}_{\tau_0}-1}(2\sqrt{\mathcal{E}}m_e(n,N_\tau)\check{p}(n) + m_e^2(n,N_\tau))$ and $m_2(N_\tau) := \sum_{\tilde{N}_{\tau_0}}^{N_T-1}(2\sqrt{\mathcal{E}}m_e(n,N_\tau)\check{p}(n) + m_e^2(n,N_\tau))$ are functions of $\check{p}(n)$ and are independent of k (i.e., independent of the transmitted symbols). Furthermore, because $\check{p}(n) = \tilde{p}_R([n+N_T-\tilde{N}_{\tau_0}]_{N_T})$ is a periodic function with period N_T and $m_e(n,N_\tau)$ is a function of $\check{p}(n)$, the summation of $m_1(N_\tau)$ and $m_2(N_\tau)$,

$$\begin{aligned}m_\xi :=& m_1(N_\tau) + m_2(N_\tau)\\ =& \sum_{n=0}^{N_T-1}\left(2\sqrt{\mathcal{E}}m_e(n,N_\tau)\check{p}(n) + m_e^2(n,N_\tau)\right),\end{aligned}$$

turns out to be a constant independent of both k and N_τ.

Next, let us consider the variance of the noise at the ADC output. Given the transmitted symbols $s(2k-2)$, $s(2k-1)$

and $s(2k)$, the variance of $\xi_1(k;N_\tau)$ can be obtained as

$$\begin{aligned}\sigma_1^2(N_\tau) &:= \text{var}\{\xi_1(k;N_\tau)\} \\ &= \sum_{n=0}^{\tilde{N}_{\tau_0}-1} \left(\text{E}\{\xi_1^2(n;k;N_\tau)\} - \text{E}^2\{\xi_1(n;k;N_\tau)\}\right),\end{aligned} \tag{16}$$

where $\xi_1(n;k;N_\tau) := \sqrt{\mathcal{E}}(s(2k-2)\nu(n+2kN_T+N_\tau) + s(2k-1)\nu(n+(2k-1)N_T+N_\tau))\check{p}(n)+\nu(n+(2k-1)N_T+N_\tau)\nu(n+2kN_T+N_\tau)$. In the analysis of the mean of noise, we have already shown that $\text{E}^2\{\xi_1(n;k;N_\tau)\}$ is independent of the transmitted symbols, and will next show that this is also true for $\text{E}\{\xi_1^2(n;k;N_\tau)\}$. Specially, we have

$$\begin{aligned}\text{E}\{\xi_1^2(n;k;N_\tau)\} &= \mathcal{E}\left(\text{E}\{\nu^2(n+(2k-1)N_T+N_\tau)\}\right. \\ &\quad \left. + 2m_e^2(n;N_\tau) + \text{E}\{\nu^2(n+2kN_T+N_\tau)\}\right)\check{p}(n) \\ &\quad + 2\sqrt{\mathcal{E}}\text{E}\{\nu^2(n+(2k-1)N_T+N_\tau)m_e(n;N_\tau) \\ &\quad + \nu^2(n+2kN_T+N_\tau)m_e(n;N_\tau)\} \\ &\quad + \text{E}\{\nu^2(n+(2k-1)N_T+N_\tau)\}\text{E}\{\nu^2(n+2kN_T+N_\tau)\},\end{aligned}$$

where $\text{E}\{\nu^2(n+kN_T+N_\tau)\} = \mathcal{N}_0/2+2\text{E}\{\gamma(n;k;N_\tau)e(n+kN_T+N_\tau)\}-2\sqrt{\mathcal{E}}s^2(k-1)\check{p}(n)m_e(n;N_\tau)+\text{E}\{e^2(n+kN_T+N_\tau)\}$.

We obtain that $\text{E}\{e^2(n+kN_T+N_\tau)\}$ and $\text{E}\{\gamma(n;k;N_\tau)e(n+kN_T+N_\tau)\}$ are both functions of $\check{p}(n)$ and independent of $s(k-1)$ when $s(k-1)$ takes values of $\{\pm 1\}$. Substituting $\text{E}\{\xi_1^2(n;k;N_\tau)\}$ to (16), we also obtain that $\sigma_1^2(N_\tau)$ is independent of the transmitted symbols, and so is true for $\sigma_2^2(N_\tau)$. Because $\check{p}(n)$ is periodic with period N_T, $\sigma_\xi^2 = \sigma_1^2(N_\tau)+\sigma_2^2(N_\tau)$ is a constant independent of N_τ and the transmitted symbols. This concludes the proof.

REFERENCES

[1] M. Abramowitz and I. A. Stegun, *Handbook of Mathematical Functions: With Formulas, Graphs, and Mathematical Tables*. New York: Dover publications, 1965.

[2] J. R. Foerster, Channel Modeling Sub-committee Report Final, IEEE P802.15-02/368r5-SG3a, IEEE P802.15 Working Group for WPAN, Nov. 2002.

[3] L. W. Hughes, "A simple upper bound on the error probability for orthogonal sinals in white noise," *IEEE Trans. Commun.*, vol. 40, no. 4, p. 670, April 1992.

[4] J.-F. Luy, T. Mueller, T. Mack, and A. Terzis, "Configurable RF receiver architectures," *IEEE Microwave Mag.*, vol. 5, no. 1, pp. 75–82, March 2004.

[5] A. B. Sripad and D. L. Snyder, "A necessary and sufficient condition for quantization errors to be uniform and white," *IEEE Trans. Signal Processing*, vol. 25, no. 5, pp. 442–448, Oct. 1977.

[6] J. Tang, Z. Xu, and B. M. Sadler, "Digital receiver for TR-UWB systems with inter-pulse interference," in *Proc. Signal Proc. Workshop on Advances in Wireless Communications*, June 2005, pp. 420–424.

[7] L. Yang and G. B. Giannakis, "Timing ultra-wideband signals with dirty templates," *IEEE Trans. Commun.*, vol. 53, no. 11, pp. 1952–1963, Nov. 2005.